Supplement of Atmos. Chem. Phys., 20, 14717–14740, 2020
https://doi.org/10.5194/acp-20-14717-2020-supplement

Atmospheric Chemistry and Physics
Open Access
EGU

Supplement of

Methane mapping, emission quantification, and attribution in two European cities: Utrecht (NL) and Hamburg (DE)

Hossein Maazallahi et al.

Correspondence to: Hossein Maazallahi (h.maazallahi@uu.nl)

Supplement

This section includes:
Supplementary Text
Supplementary Tables S1 to S14
Supplementary Figures S1 to S19
In this section the supporting documents related to the measurements and data evaluation are provided.

Table of Contents

List of Tables

List of Figures

Acronyms, Chemical Symbols and Scientific Units

ACM	Authority for Consumers and Markets in the Netherlands
bcm	billion cubic meters
°C	degree Celsius
C_2:C_1	Ethane to Methane Enhancements Ratio
C_2H_6	Ethane
CCAC	Climate and Clean Air Coalition
CH_4	Methane
CO_2	Carbon Dioxide
CSU	Colorado State University
DBI GUT Leipzig	DBI Gas- und Umwelttechnik GmbH Leipzig
DE	Deutschland
DVGW	Deutscher Verein des Gas-und Wasserfaches
EDF	Environmental Defense Fund
EIA	Energy Information Administration
GHG	Greenhouse Gas
GIS	Geographic Information System
GPDM	Gaussian Plume Dispersion Model
GPS	Global Positioning System
H_2O	Water
Hz	Hertz
ICOS	Integrated Carbon Observation System
IMAU	Institute for Marine and Atmospheric research Utrecht
KNMI	Koninklijk Nederlands Meteorologisch Instituut
L	Liter
LBEG	Landesamt für Bergbau, Energie und Geologie
LDC	Local Distribution Company (for natural gas consumption)
LI	Leak Indication: spatially clustered and temporally aggregated locations of methane enhancements which are >10 % above background level
mbar	millibar
ml	milliliter
MEMO^2	Methane goes Mobile–Measurements and Modelling
MI	Meteorological Institute
MPI-Met	Max-Planck Institute for Meteorology
NGDN	Natural Gas Distribution Network
NL	The Netherlands
OH	Hydroxyl radical
OSM	Open Street Map
ppb	parts per billion
ppm	parts per million
RHUL	Royal Holloway University of London
RIVM	Rijksinstituut voor Volksgezondheid en Milieu
t	tons
u	wind speed
UBA	Umweltbundesamt
UU	Utrecht University
US	The United States
UTC	Coordinated Universal Time
V	volts
WWTP	Waste Water Treatment Plant
yr	Year
$\delta^{13}C$	$\delta^{13}C$-CH_4
δD	$\delta^{2}H$-CH_4
σ_y	horizontal plume dispersion coefficient
σ_z	vertical plume dispersion coefficient

S.1) Data collection and instrumentation

S.1.1) Mobile measurements

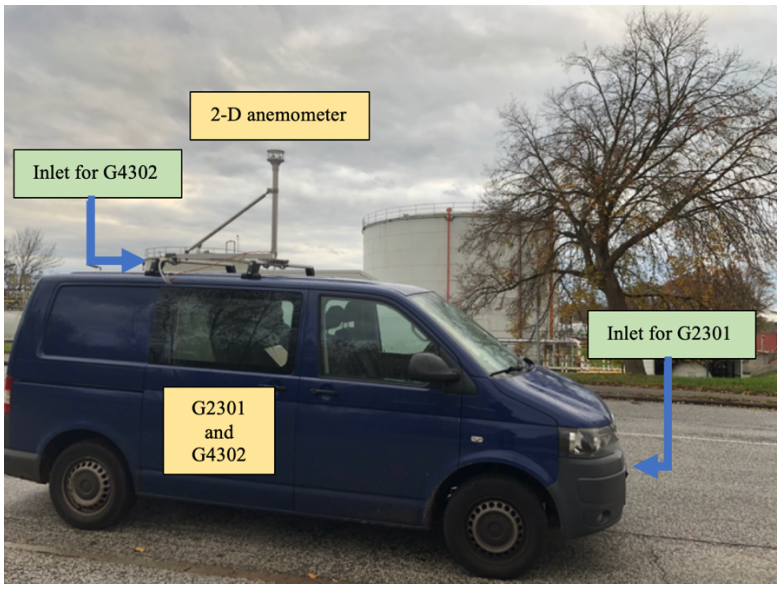

Figure S1: Mobile measurement platform

S.1.2) Target cities

Figure S2a and Figure S2b show total length of roads driven in Utrecht (≈ 1,300 km) and Hamburg (≈ 2,500 km). The areas outlined in black are the city areas where LIs from the NGDN were evaluated.

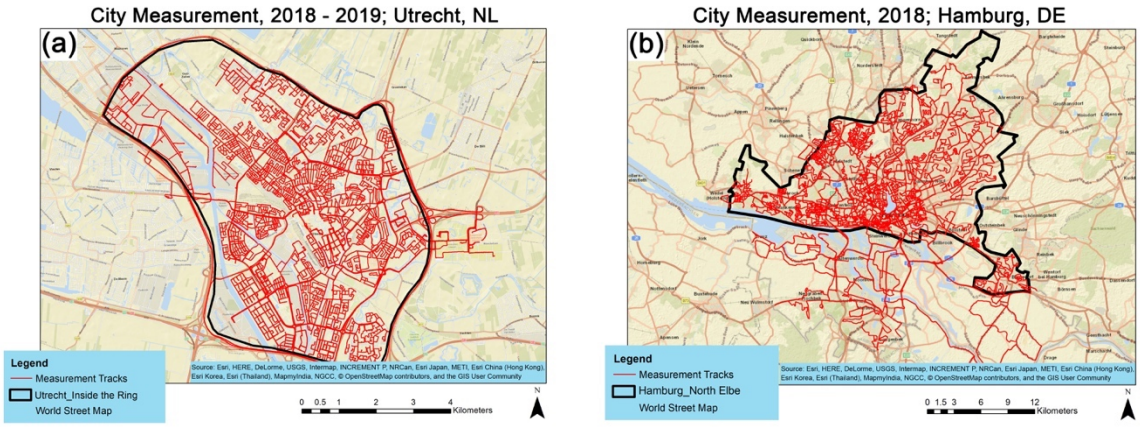

Figure S2: Mobile measurement in (a) Utrecht and (b) Hamburg

Table S1 and Table S2 provide information on each day's survey dates, districts targeted, instruments on-board, and duration of mobile measurements during each individual measurement days.

Table S1: Information about each day's mobile measurement surveys in Utrecht

Date dd.mm.yyyy	Picarro G2301		Picarro G4302		Target District	km driven	Km driven inside the ring
	Availability	Time correction	Availability	Time correction			
20.02.2018	Yes	14	-	-	Kanaleneiland	48.2	46.4
25.02.2018	Yes	14	-	-	Oud Hoograven, Hoograven, Lunette, and Hoograven,	53.2	50.5
26.02.2018	Yes	14	-	-	Tolsteeg	31.8	29.2
27.02.2018	Yes	14	-	-	Rivierenwijk	28.6	26.0
01.03.2018	Yes	14	-	-	Lombok, Nieuw Engeland, Oog in Al, and Halve Maan	72.2	69.8
12.03.2018	Yes	14	-	-	Rubenslaan, Schildersbuurt, Rijnsweerd, Tuindorp, and the Waste Water Treatment Plant	68.7	64.1
13.03.2018	Yes	14	-	-	Zeeheldenbuurt Hengeveldstraat, Rijnsweerd Noord, Wittevrouwen, Buiten Wittevrouwen, and Oudwijk	51	45.8
14.03.2018	Yes	14	-	-	Overvecht, Wolga- en Donaudreef, Taag- en Rubicondreef, Tigris- en Bostondreef, Schaakbuurt, and Geuzenwijk	123.9	119.6
15.03.2018	Yes	14	-	-	Lauwerecht, Pijlsweerd-Zuid, Tweede Daalsebuurt, Egelantierstraat-Mariëndaalstraat, Het Kleine Wijk, and Waste Water Treatment Plant	51.9	42.3
23.04.2018	Yes	14	-	-	Zuilen-Noord, Prins Bernhardplein, and Elinkwijk,	45.6	25.2
24.04.2018	Yes	14	-	-	Elinkwijk, Schepenbuurt bedrijvengebied Cartesiusweg, Dichterswijk, City Centre (Lange Nieuwstraat, Hooch Boulandt Moreelsepark, Wijk C, Breedstraatbuurt, Nobelstraat) and Waste Water Treatment Plant	204.4	117.1
25.04.2018	Yes	14	-	-	Blauwkapel and Voordorp en Voorveldsepolder	25.5	23.3
26.04.2018	Yes	14	-	-	Transwijk-Noord, Bedrijvengebied Kanaleneiland, and Bedrijventerrein De Wetering	100.5	94.0
29.04.2018	Yes	14	-	-	Bedrijventerrein Lageweide, Bedrijvengebied Overvecht, Wijk C, Rijnsweerd Noord, Waste Water Treatment Plant, and City Rings	36.3	33.9
09.05.2018	Yes	14	-	-	Hoograven-Zuid, Kanaleneiland, and Waste Water Treatment Plant	53.3	39.0
07.01.2019	Yes	28	-	-	Kanaleneiland and Waste Water Treatment Plant	38.4	30.4
14.02.2019	Yes	28	Yes	108	City Centre (Lange Nieuwstraat, Hooch Boulandt Moreelsepark, Wijk C, Breedstraatbuurt, Nobelstraat)	54.7	52.2
15.02.2019	Yes	28	Yes	108	Kanaleneiland	63.2	60.0
24.04.2019	Yes	28	Yes	220	City Centre, Kardinaal de Jongweg and Kanaleneiland	39.2	23.1
04.06.2019	Yes	21	Yes	220	Joseph Haydnlaan, Westbroek, and Waste Water Treatment Plant	68.1	18.8

Table S2: Information about each day's mobile measurement surveys in Hamburg

Date dd.mm.yyyy	Picarro G2301		Picarro G4302		Target District	km driven	Km driven north Elbe
	Availability	Time correction	Availability	Time correction			
18.10.2018	Yes	28	Yes	212	Harbor	50.9	13.7
19.10.2018	Yes	28	Yes	212	Harbor and oil extraction site	125.39	18.39
20.10.2018	Yes	28	Yes	212	Rotherbaum, Hoheluft-West, and Lokstedt	76.2	76.2
22.10.2018	Yes	28	Yes	217	Niendorf	89.3	89.3
24.10.2018	Yes	28	Yes	218	Schnelsen and Eidelstedt-West	98.8	91.6
25.10.2018	Yes	28	Yes	218	Harbor	122.6	12.6
26.10.2018	Yes	28	-	-	Groß Flottbek	47.1	47.1
27.10.2018	Yes	28	Yes	220	City Centre	74.2	72.3
28.10.2018	Yes	28	Yes	220	Altona	80.9	80.9
29.10.2018	Yes	28	Yes	220	Othmarschen-West, Nienstedten-East	66.8	66.8
30.10.2018	Yes	28	Yes	220	Blankenese, Sülldorf, and Rissen	137.6	132.4
31.10.2018	Yes	28	Yes	226	St. Georg, Hamburg-Hamm, Hohenfelde, Eilbek, and Barmbek-Süd	99.5	99.5
01.11.2018	Yes	28	Yes	227	Rahlstedt, Wandsbek, and Billstedt	156.5	154.8
02.11.2018	Yes	28	Yes	228	Sasel, Bergstedt, and Bramfeld,	111.3	111.3
03.11.2018	Yes	28	Yes	229	Barmbek-Süd, Winterhude, and Barmbek-Nord	82.7	82.7
04.11.2018	Yes	28	Yes	230	Hamburg-Nord, Hummelsbüttel, Langenhorn, Lemsahl-Mellingstedt, Duvenstedt, and Wohldorf-Ohlstedt	201.7	192.5
06.11.2018	Yes	28	Yes	236	Eimsbüttel, Lokstedt, Winterhude-North, Rotherbaum-West, and Schnelsen	114.6	114.6
07.11.2018	Yes	28	Yes	236	Harbor and Sampling	93.2	12.2
08.11.2018	Yes	28	Yes	236	Sampling	81.7	76.4
09.11.2018	Yes	28	Yes	236	Sampling	122.9	43.5
10.11.2018	Yes	28	Yes	236	Lurup, Groß Flottbek – NorthWest, Marmstorf, Neugraben-Fischbek, Harburg, and Ronneburg	171.6	78.7
11.11.2018	Yes	28	Yes	240	Bergedorf, Allermöhe, Lohbrügge,	175.1	88.5
14.11.2018	Yes	28	Yes	245	East-West Transects on the North Side of the Elbe River	87.4	72.6

S.1.3) Instruments comparison

In the Hamburg study, the two analyzers (G2301 and G4302) were operated in parallel. The Picarro G2301 instrument measures methane (CH_4), carbon dioxide (CO_2), and water vapor (H_2O) and provides 0.3 Hz measurements at a flow rate of about 200 ml min^{-1} and the G4302 measures CH_4, ethane (C_2H_6), and H_2O with a frequency of 1 Hz and at a flow rate of about 2 L min^{-1}. The G4302 can be operated in CH_4 only mode, or in C_2H_6 – CH_4 mode, where the noise of CH_4 measurements increases by about one order of magnitude. The inlet for the Picarro G2301 instrument was from the bumper while the inlet for the G4302 was from the roof of the vehicle (Figure S1). In Figure S3c and Figure S3d linear correlation of methane mole fractions shows a correlation of results from the G2301 and G4302 instruments, the latter in both C_2H_6 and CH_4-only mode, which show good linear correlation in both modes. In order to guarantee consistency with the von Fischer et al., (2017) and Weller et al., (2019) quantification algorithm which was developed for a G2301 instrument, in our study the data from this instrument are used for the CH_4 quantification and attribution through CH_4:CO_2 ratio, and the G4302 is primarily used for source attribution via the C_2H_6:CH_4 ratio (C_2:C_1).

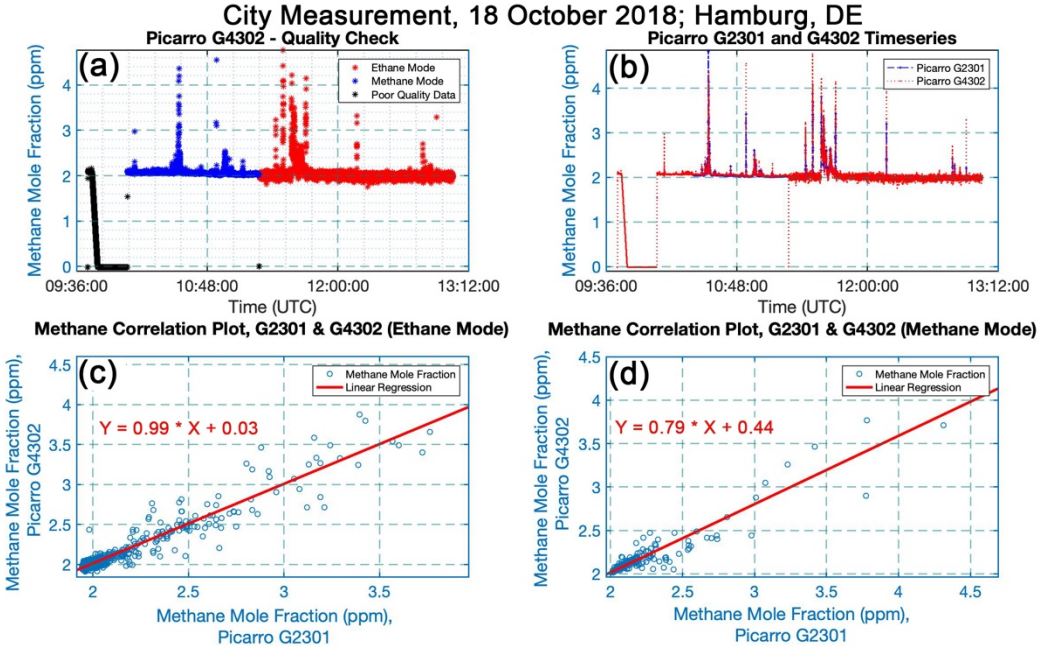

Figure S3: (a) Example of raw data and data quality check of G4302, (b) timeseries of CH_4 mole fraction recorded by G2301 and G4302, (c) in-situ measurement correlation plot of G2301 and G4302 while the G4302 was in ethane mode, and (d) in-situ measurement correlation plot of G2301 and G4302 while the G4302 was in methane mode

Table S3 shows a comparison between the different instruments and inlets for a selection of CH_4 enhancements where the G4302 operated in CH_4 mode. CH_4 enhancements above background level are referred to leak indications (LIs). All the LIs were observed by both instruments when both instruments were running together. In a few cases, the G4302 places an LI in a higher category (when using the Weller et al., (2019) algorithm). The largest difference between the two instruments was observed for the highest LI in Utrecht, where a CH_4 enhancement of 16.2 ppm (corresponding to 100 L min^{-1}) was recorded on the G2301 instrument, whereas an enhancement of 31.9 ppm (corresponding to 230 L min^{-1}) was recorded by the G4302. The difference may be due to the higher flow rate and sampling rate of the G4302, which reduces smoothing in the sample cell compared to the G2301 instrument. However, the difference may also be due to the two different inlets sampling different parts of the plume, because of the different inlet location. In principle, the expected behavior would then be opposite: Larger enhancements would be expected closer to the ground where the inlet of the G2301 instrument

is located, but turbulent plume dispersion in on streets by driving cars can result in very irregularly shaped emission plumes.

Table S3: Comparison of enhancements detected with the G2301 and G4302 instruments

Instrument	Yellow category (0.5 – 6 L min^{-1} emissions)	Orange category (6 – 40 L min^{-1} emissions)	Red Category (>40 L min^{-1} emissions)	Total	Sum Emissions (L min^{-1})
Hamburg					
G2301	90	8	2	100	370
G4302	86	12	2	100	400
Utrecht					
G2301	22	3	1	26	180
G4302	20	5	1	26	370*

* The large difference is primarily due to the much higher CH4 elevation recorded with the G4302 for the LI in the "red" category, see text.

S.1.4) Road data from Open Street Map (OSM)

Information from the Open Street Map (OSM) (Figure 1) was used for several purposes. Firstly, it was investigated whether there is any correlation between type of roads and CH_4 enhancements. Therefore, the streets in both cities were categorized into level 1, 2, 3, residential, and unclassified streets based on the categories from the OSM (Table S4). Secondly, not all streets across the cities were covered and data on the total road network from OSM were used to extrapolate the results from the roads covered to the entire natural gas distribution network in the cities. The OSM was also used to determine from the recorded GPS coordinates how many times each street was surveyed. As GPS coordinates may not perfectly sit on OSM data, 15m both-sided buffer zone was used for level 1, 2, and 3 and 10m both-sided buffer zone was used to extract driven streets out of OSM data. These distances are slightly smaller than used for the US cities, reflecting the denser infrastructure and street network in Utrecht and Hamburg.

S.1.5) Road visits

Table S4: Road category visits

	Inside the ring, Utrecht			North Elbe, Hamburg		
Road class	Total (km)	Once (km)	More than Once (km)	Total (km)	Once (km)	More than Once (km)
Level 1	37.4	9.0	28.4	160.5	92.5	68.0
Level 2	45.4	12.0	33.4	197.8	124.2	73.6
Level 3	43.5	14.8	28.7	194.3	142.5	51.8
Residential	246.8	146.8	100.0	619.6	509.6	110.0
Unclassified	81.7	48.7	33.0	50.5	35.7	14.8

S.1.6) Measurements from facilities

Table S5: Measurement from the waste water treatment plant in Utrecht (52.109791° N, 5.107605° E)

No.	Date (dd.mm.yyyy)	Wind Direction (°)	Wind Speed (m s^{-1})
1	12.03.2018	200 ± 5	3.7 ± 1.1
2	24.04.2018	210 ± 5	4.0 ± 1.2
3	07.01.2019	178 ± 5	3.5 ± 1.1

Table S6: CH_4 measurements from facilities in Hamburg

Facility	Date dd.mm.yyyy	Lat (° N)	Lon (° E)	Time Start (UTC) hh:mm:ss	Time End (UTC) hh:mm:ss	Wind Direction (°)	Wind Speed (m s^{-1})
A) Tank Reserves	18.10.2018	53.493237	9.969307	11:25:43	12:10:46	342 ± 9.5	3.2 ± 1.0
B) Refinery	18.10.2018	Unknown	Unknown	11:00:01	11:11:48	328 ± 4.3	3.2 ± 1.0
B) Refinery	20.10.2018	Unknown	Unknown	13:47:00	13:49:21	289.8 ± 3.3	4.7 ± 1.4
C) Steel factory	25.10.2018	53.519042	9.906555	12:42:54	13:15:54	288.7 ± 3.3	7.0 ± 2.1
C) Steel factory	07.11.2018	53.519042	9.906555	11:44:46	12:31:04	153.7 ± 9.8	1.4 ± 0.4
C) Steel factory	09.11.2018	53.519042	9.906555	09:59:41	10:22:23	109.5 ± 6.4	1.8 ± 0.5
D1) Separator	19.10.2018	53.468829	10.184400	08:42:11	08:42:36	323.5 ± 25.4	1.0 ± 0.3
D2) Storage Tank	19.10.2018	53.468446	10.187410	08:41:44	10:04:36	323.5 ± 25.4	1.0 ± 0.3

D3) Extraction Well	19.10.2018	53.466709	10.180733	08:41:44	10:04:36	323.5 ± 25.4	1.0 ± 0.3
D2) Storage Tank	11.11.2018	53.468446	10.187410	14:02:53	14:28:08	175 ± 1.4	2.7 ± 0.8
E) Farm	11.11.2018	53.444276	10.226374	14:34:30	15:07:49	174 ± 1.6	2.5 ± 0.8
F) Compost and Soil Company	04.11.2018	53.680233	10.053751	14:44:34	15:29:26	112 ± 3.1	1.5 ± 0.5
G) Landfill	04.11.2018	53.690721	10.092599	09:42:58	10:00:52	124 ± 3.2	2.4 ± 0.7
H) Car manufacturing factory	07.11.2018	53.475618	9.925336	14:28:41	14:40:29	171.5 ± 3.8	0.8 ± 0.2

Figure S4: Construction at the street level; (a) not possible to access the total width or (b) streets were completely blocked

S.1.7) Revisits; example of Utrecht city centre

In Figure S5, one of the revisit surveys across Utrecht is shown in which the city centre was revisited after about 10 months.

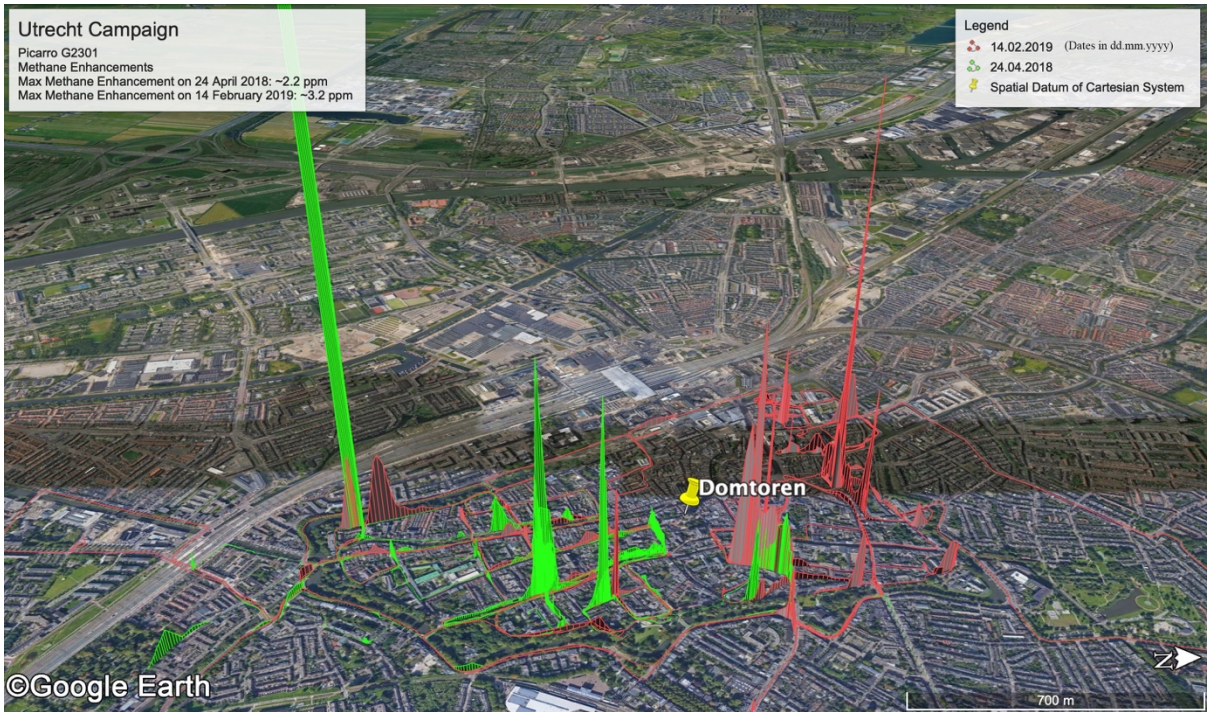

Figure S5: Mobile measurement across city centre of Utrecht in February 2018 (red) and April 2019 (green)

S.1.8) Air sample collection

Samples were taken either inside the car or outside depending on road accessibility. Sampling locations were selected guided by the LIs observed during the untargeted surveys (Table S1 and Table S2). As the delay time of G4302 reading was lower and the analyzer is portable, it was more practical to use this instrument for sampling. In Figure S6a, M. M. is taking samples at a location where the car could stop at the LI locations. In Figure S6b, J. M. F. is walking with the G4302 analyzer to locate a source, in this case the source is shown in Figure S15.

Figure S6: Taking samples (a) inside the car or (a) outside

S.2) Data evaluation procedures of CH_4 quantification

S.2.1) Background extraction

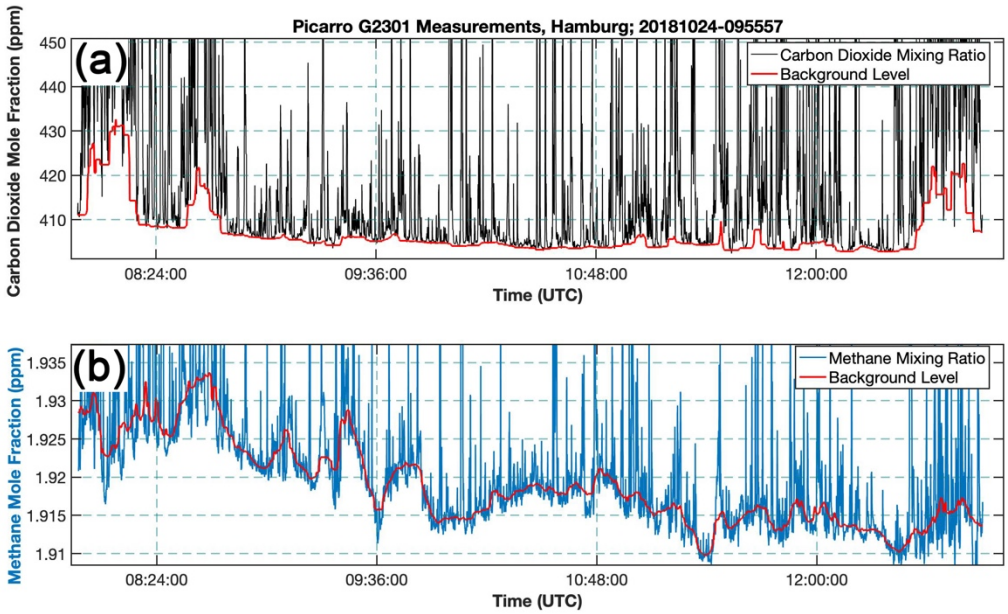

Figure S7: Background extraction of (a) CO_2 and (b) CH_4; example of a survey in Hamburg

S.2.2) Quantification of emissions from leak indications

The evaluation procedure was established by von Fischer et al. (2017) and Weller et al., (2019) for the G2301 instrument, so we used the dataset from G2301 for standard evaluation of LIs. Figure S8 shows the overview of CH_4 emission quantification steps for emissions from the natural gas distribution network.

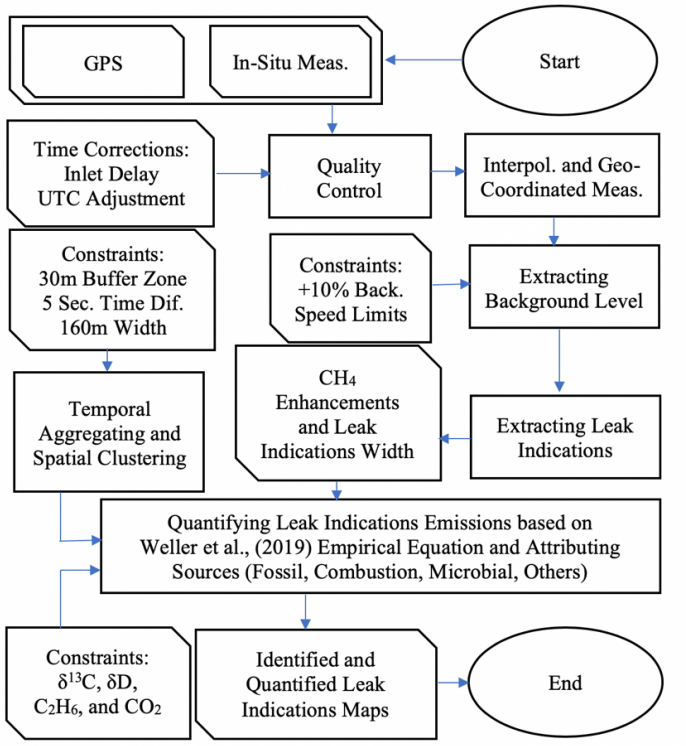

Figure S8: Flow diagrams for the evaluating CH_4 emissions of leak indications

S.2.3) Cartesian system and clustering

GPS records logged in decimal degrees were converted to a Cartesian coordinate system for further LI clustering using Eq. (S1). For this, local geographical datums were defined in both cities, in Utrecht it was the city cathedral (Domtoren) and in Hamburg the St. Nicholas' Church (Table S7). The location of a point i relative to the reference point was calculated as:

$$X(i) = (\text{Longitude (i)} - \text{Longitude (Ref)}) * \frac{\pi}{180} * \cos\left(\frac{Latitude\ (Ref) * \pi}{180}\right) * R_e \quad \text{(S1a)}$$

$$Y(i) = (\text{Latitude (i)} - \text{Latitude (Ref)}) \frac{\pi}{180} * R_e \quad \text{(S1b)}$$

where Re = $6.378*10^6$ m is the radius of the Earth.

Table S7: Local geographical datums in Utrecht and Hamburg

City	Location	Latitude (° N)	Longitude (° E)
Utrecht	Domtoren	52.090628	5.121310
Hamburg	St. Nicholas' Church	53.547479	9.990709

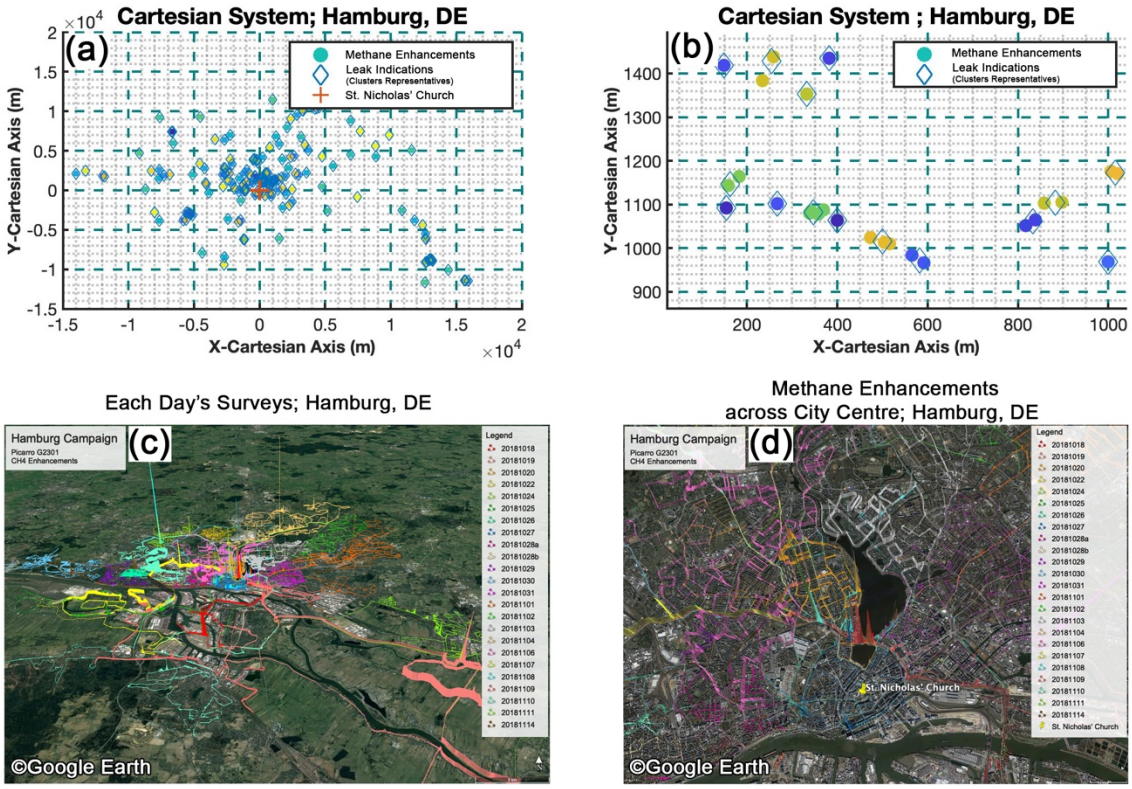

Figure S9: Emission locations and clusters. (a) All LIs and clusters in the target area, (b) LIs and clusters in a smaller region, (c) complete view of each day's surveys across Hamburg, and (d) focus of each day's surveys across city centre of Hamburg

S.2.4) Code comparison with CSU

Figure S10 shows a comparison of results obtained with the MATLAB code from Utrecht University (UU) (Maazallahi et al., 2020) with the code that was used by Colorado State University (CSU) for US cities. The two evaluation systems return basically very similar results.

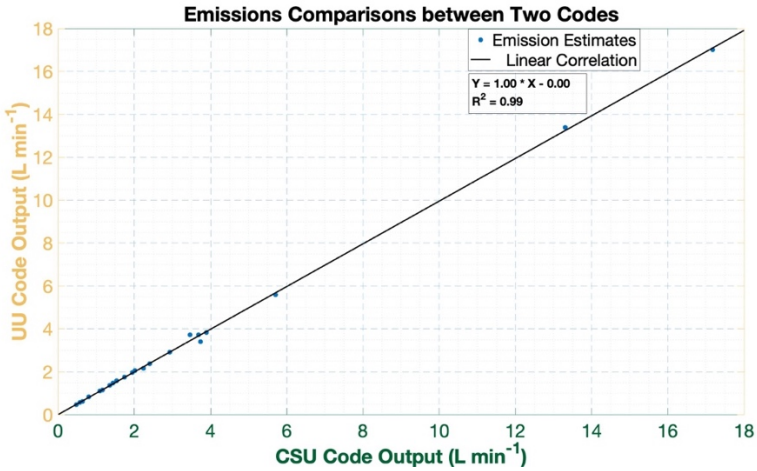

Figure S10: Comparison of evaluation code from UU and CSU

We adopt the distribution of observed CH_4 enhancements into different LI categories according to von Fischer et al., (2017).

S.2.5) Quantification of emissions from facilities

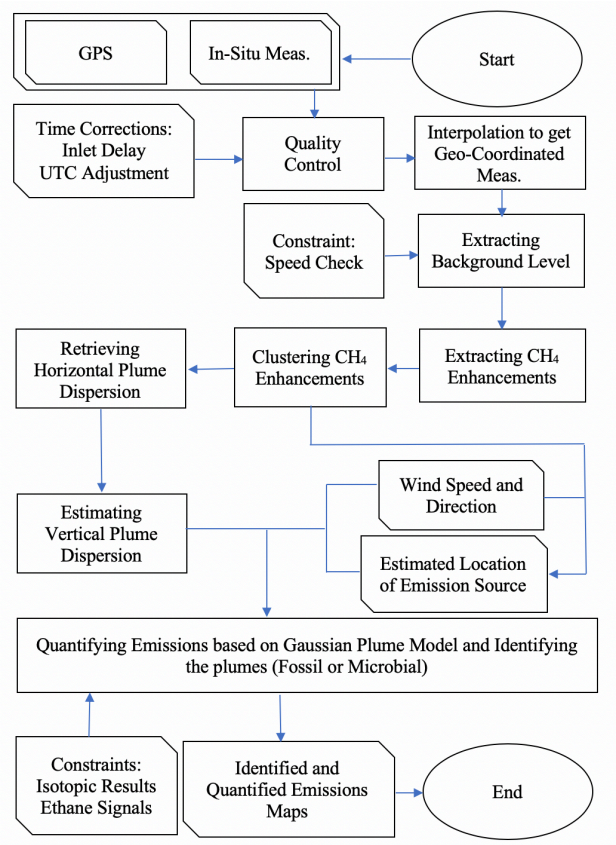

Figure S11: Flow diagrams for the evaluating CH_4 emissions of facilities

There are considerable difficulties and uncertainties in quantifying CH_4 emissions from facilities. Finding suitable roads that allow application of the Gaussian Plume Dispersion Model (GPDM) technique downwind of the source is often challenging. In addition, the characteristics of the sources are often complex. Waste water treatment plants like the one in Utrecht consist of several water tanks, but in the GPDM the whole plant was considered as one-point source. The same applies to the Compost and Soil Company and water-oil separator in Hamburg. Changing the distance from the source along the x-axis in GPDM analysis results in changes in σ_z, and for the case shown in Figure 7 $\sigma_z = 32.1 \pm 14.2$ m. Errors in wind speed are estimated to be ± 30 % and for wind direction ± 5°. These errors are included in the total error estimate. The uncertainty in the height of the CH_4 emission is most relevant for the case of the storage tank in Hamburg. Most likely, emissions are from the top of tanks, but there can also be emissions at ground level. In addition, vertically stable atmospheric conditions or larger turbulences may lead to transport of air from a higher emission point to the ground level. In the simple GPDM, emission estimates rise exponentially when the point of emission is elevated. E.g. by changing source emission height from 0 - 10 m for the storage tank in Hamburg, the emission rate would change from 3.4 to 10.6 t yr^{-1}.

Emissions from facilities show significant contributions to the total emissions in both cities. This highlights the importance of considering emissions from all possible sources within a boundary of an study area. Hopkins et al. (2016) showed that more than 30 % of emissions from Los Angeles basin were not accounted in the emission inventory which are due to widely spread sources and mostly originate from fugitive fossil fuel emissions.

S.2.6) Unintended measurements

Figure S12 shows measurements during a period when the measurement vehicle followed a car exhausting black smoke. Black smoke is an indication for incomplete internal combustion of the vehicle. In Figure S12, the ratio of the area under the CH_4 enhancements along the driving track (in ppb*m) to the area of CO_2 enhancements along the driving track (in ppm*m) is 5.5 ppb:ppm which is much higher than reported in previous studies, possibly indicating incomplete combustion.

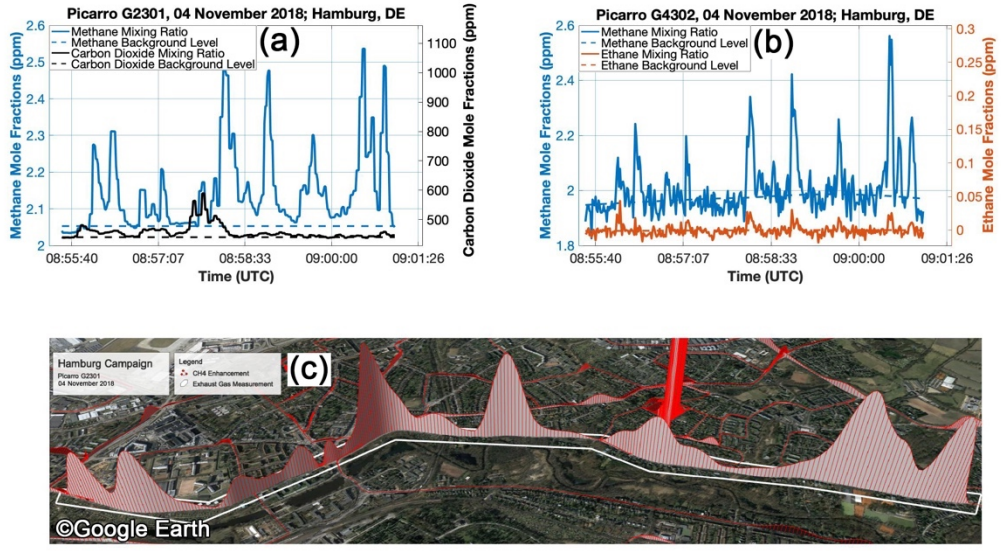

Figure S12: Exhaust measurement from a car; (a) timeseries of CH_4 and CO_2 mole fractions from G2301, (b) timeseries of CH_4 and C_2H_6 mole fractions from G4302, and (c) the CH_4 excess track of measurement while following the car

S.2.7) Data evaluation procedures of isotopic analysis

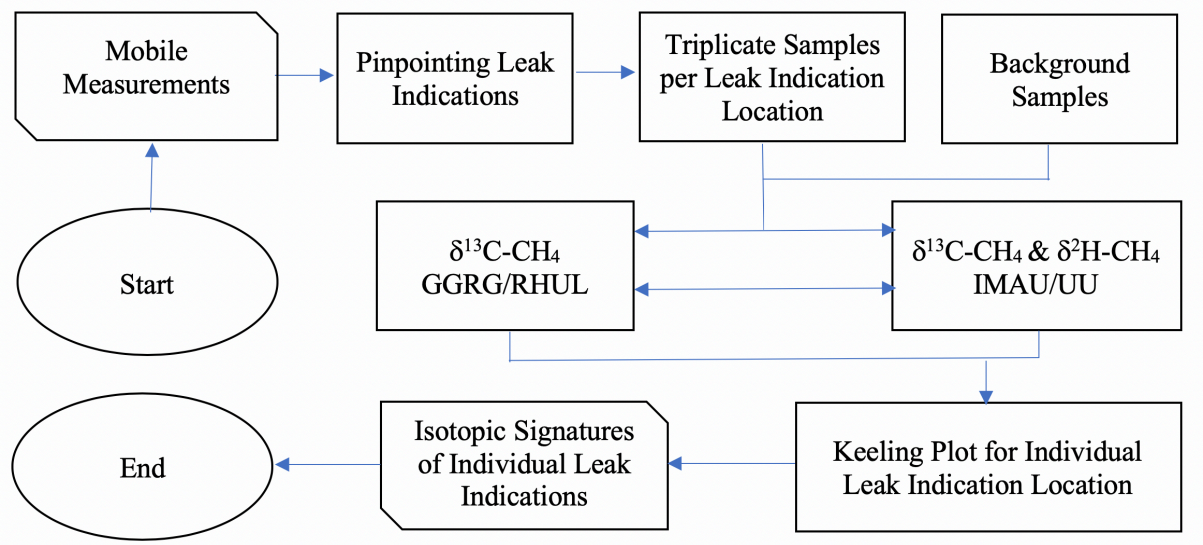

Figure S13: Flow diagram for isotope analysis

S.3) Evaluations outcomes

S.3.1) Methane emission distribution over different road categories

Table S8: Statistics of observed LIs for different street categories in Hamburg and Utrecht. The three values per cell are the number of LIs, the total emission rate from all LIs in this category and the emission rate per LI

		Total	Visited once	Visited more than once
Level 1				
Utrecht (Inside the Ring)	Number	6 LIs	----	6 LIs
	Emissions	4.6 L min^{-1}	----	4.6 L min^{-1}
	Emissions per LI	0.76 L/min/LI	----	0.76 L/min/LI
Hamburg (North Elbe)	Number	29 LIs	10 LIs	19 LIs
	Emissions	68.1 L min^{-1}	15.5 L min^{-1}	52.7 L min^{-1}
	Emissions per LI	2.3 L/min/LI	1.5 L/min/LI	2.8 L/min/LI
Level 2				
Utrecht (Inside the Ring)	Number	16 LIs	2 LIs	14 LIs
	Emissions	144.7 L min^{-1}	6.4 L min^{-1}	138.3 L min^{-1}
	Emissions per LI	9.0 L/min/LI	3.2 L/min/LI	9.9 L/min/LI
Hamburg (North Elbe)	Number	34 LIs	2 LIs	32 LIs
	Emissions	99.4 L min^{-1}	1.5 L/min	97.94 L min^{-1}
	Emissions per LI	2.9 L/min/LI	0.7 L/min/LI	3.1 L/min/LI
Level 3				
Utrecht (Inside the Ring)	Number	3 LIs	1 LI	2 LIs
	Emissions	10.2 L min^{-1}	1.6 L min^{-1}	8.6 L min^{-1}
	Emissions per LI	3.4 L min^{-1} LI^{-1}	1.6 L min^{-1} LI^{-1}	4.3 L min^{-1} LI^{-1}
Hamburg (North Elbe)	Number	23 LIs	8 LIs	15 LIs
	Emissions	43.0 L min^{-1}	7.6 L min^{-1}	35.4 L min^{-1}
	Emissions per LI	1.9 L min^{-1} LI^{-1}	1.0 L min^{-1} LI^{-1}	2.4 L min^{-1} LI^{-1}
Residential				
Utrecht (Inside the Ring)	Number	45 LIs	8 LIs	37 LIs
	Emissions	92.7 L min^{-1}	12.6 L min^{-1}	80.1 L min^{-1}
	Emissions per LI	2.1 L min^{-1} LI^{-1}	1.6 L min^{-1} LI^{-1}	2.2 L min^{-1} LI^{-1}
	Number	52 LIs	23 LIs	29 LIs
	Emissions	273.8 L min^{-1}	41.8 L min^{-1}	232.1 L min^{-1}
	Emissions per LI	5.3 L min^{-1} LI^{-1}	1.8 L min^{-1} LI^{-1}	8.0 L min^{-1} LI^{-1}
Unclassified				
Utrecht (Inside the Ring)	Number	11 LIs	5 LIs	6 LIs
	Emissions	37.8 L min^{-1}	13.4 L min^{-1}	24.4 L min^{-1}
	Emissions per LI	3.4 L min^{-1} LI^{-1}	2.7 L min^{-1} LI^{-1}	4.1 L min^{-1} LI^{-1}
Hamburg (North Elbe)	Number	7 LIs	2 LIs	5 LIs
	Emissions	5.9 L min^{-1}	1.5 L min^{-1}	4.4 L min^{-1}
	Emissions per LI	0.8 L min^{-1} LI^{-1}	0.8 L min^{-1} LI^{-1}	0.9 L min^{-1} LI^{-1}

S.3.2) Emission per capita

Per-capita emissions in both cities were based on the LandScan data, which use remote sensing imagery and analysis of nighttime lights, land cover and road proximity at ≈1 km^2 (30" * 30") spatial resolution (Bright et al., 2000) to estimate population density. The LandScan data yield 0.28 and 1.45 million inhabitants in the study area of Utrecht and Hamburg respectively (Figure S14).

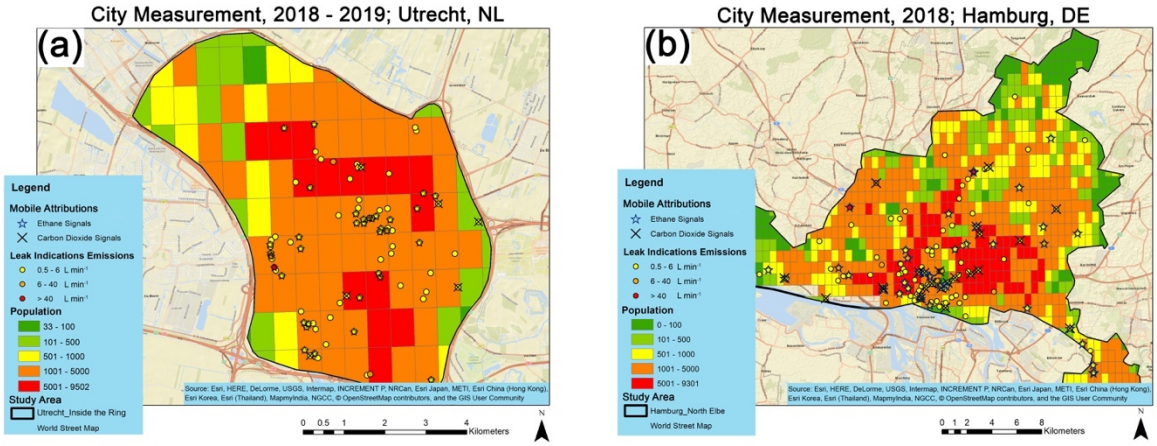

Figure S14: Population distribution in (a) Utrecht and (b) Hamburg

S.3.3) Isotopic signature and ethane/methane ratio

Table S9: Isotopic signature and ethane/methane (C_2:C_1) ratio; North Elbe area in Hamburg

No.	Latitude (° N)	Longitude (° E)	Location	$\delta^{13}C$	δD	C_2:C_1 (%)	Emission (L min^{-1})
1	53.5605556	9.99483722	Warburgstrasse	-50.4	-278.5	0	7.6
2	53.577521	9.988869	Rothenbaumchaussee	-62.7	-258	0	1.9
3	53.567191	9.999819	Alte Rabenstrasse	-52.19	-317.9	0	7.5
4	53.557113	9.996773	Lombardsbrücke	-46.3	-344.6	0	11.4
5	53.548297	9.973536	Neumayerstrasse	-49.9	-315.6	0	15.0
6	53.558212	10.006785	An der Alster	-23.4	-152.5	0	1.8
7	53.582506	10.016915	Geibelstrasse	-40.7	-194.2	3.0 ± 1.0	1.6
8	53.63921	10.040574	Distelweg	-42.6	-206.8	1.5 ± 0.5	46.6
9	53.614763	9.892181	Halstenbekerweg	-43.3	-187	3.6 ± 1.5	1.7
10	53.61402	9.890026	Astweg	-41.9	-185.1	3.6 ± 1.5	98.1
11	53.5631395	9.9862702	Edmund-Siemers Allee	-41.2	-207.4	3.8 ± 0.7	19.5
12	53.5836695	9.9839906	Eppendorfer Baum	-51.1	-301.3	0	2.0
13	53.5431789	10.0255373	Amsinckstrasse+Süderstrasse	-53.6	-272.7	0	1.6

Table S10: Isotopic signature and C_2:C_1 ratio from facilities in Hamburg

No.	Date dd.mm.yyyy	Latitude (° N)	Longitude (° E)	Location	Wind Direction	$\delta^{13}C$	δD	C2:C1
1	04.11.2018	53.68281	10.046241	Hummelsbütteler Steindamm (F)	112 ± 3.1	-46.9	-265.4	0
2	10.11.2018	53.572974	9.898723	Luruper Chaussee; Sudden wide plume	155.9 ± 10.1	-62.6	-287.8	0
3	09.11.2018	53.541798	9.917605	The New Elbe Tunnel	111.7 ± 6.3	-28.6	-176.2	---
4	09.11.2018	53.51684	9.91380075	Steel factory; Dradenaustrasse (C)	109.5 ± 6.4	-50.1	-228.2	4.6 ± 1.9
	09.11.2018	53.5214485	9.90923915	Steel factory; Dradenaustrasse (C)	109.5 ± 6.4	-49.5	-269.9	---
5	18.10.2018	53.49147	9.97216	Oil storage tanks (A)	342 ± 9.5	-48.3	-421.7	0
6	07.11.2018	53.47645	9.924026	Mercedesstraße (H)	171.5 ± 3.8	-43.0	-207.3	2.4 ± 0.6
7	19.10.2018	53.40675	10.13535	Big Plume; Steller Chaussee	290 ± 29.5	-66.0	-101.9	---
8	11.11.2018	53.445221	10.228102	Farm; Neuengammer Hausdeich	174 ± 1.6	-57.0	-317.2	0
9	19.10.2018	53.46275	10.18198	Neuengammer	323.5 ± 25.4	-53.0	-235.8	-----
	19.10.2018	53.467774	10.19001	Oil Storage Tank; Randerseidet schleusendam (D2)	323.5 ± 25.4	-45.6	-164	6.6 ± 1.4
	11.11.2018	53.469045	10.188069	Oil Storage Tank; Neuengammer Hausdeich (D2)	175 ± 1.4	-44.8	-183.2	7.7 ± 1.5

Figure S15: (a) CH_4 enhancements in the southern part of the Alster in Hamburg, the LIs inside the white polygon were attributed to a microbial source, and (b) the photograph shows an exhaust from the sewage system that was identified as strong CH_4 source

S.3.4) Measurements inside the New Elbe Tunnel

During three surveys (07, 09, and 10 - November 2018), we drove inside the new Elbe tunnel to reach the south side of the Elbe river. Figure S16a-c show the CO_2 and CH_4 measurement time series during these passages, and Figure S16d shows a correlation of CO_2 and CH_4 enhancements above the background. The average CH_4:CO_2 enhancement ratio inside the tunnel was 0.2 ± 0.1 ppb:ppm which is in agreement with the ratio of 0.3 reported by Naus et al. (2018) for cars working under normal conditions.

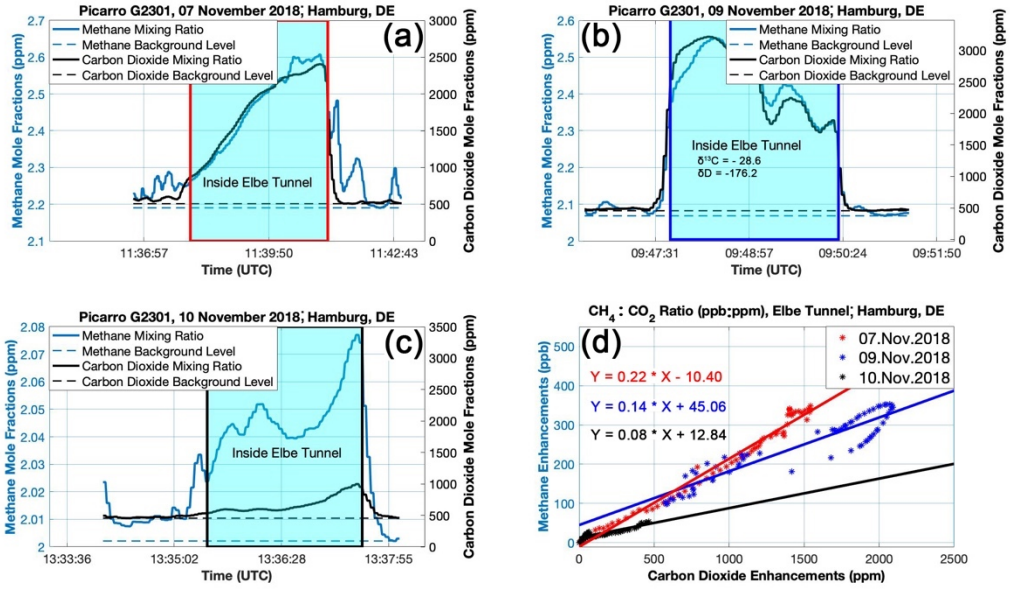

Figure S16: In situ measurements from G2301 during driving inside the new Elbe tunnel; (a) on 07 November 2018, (b) on 09 November 2018 including signatures from isotopic sampling analysis, (c) on 10 November 2018, and (d) CH_4:CO_2 ratio of enhancements inside the tunnel

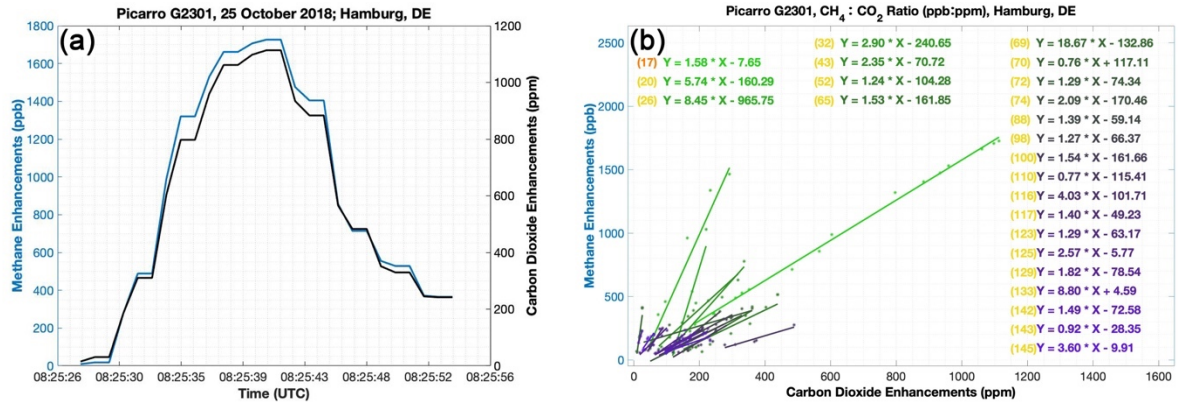

Figure S17: (a) Example of concomitant CH_4 and CO_2 enhancements for a LI measured with the G2301 instrument and (b) CH_4 and CO_2 correlations for the LIs attributed to combustion sources in Hamburg

S.4) Standards, regulations, and LDC leak detection

S.4.1) Standards and regulations for local gas companies in Germany

In this section, technical regulations on inspection of gas pipework systems with operation pressures up to 16 bar by Deutscher Verein des Gas- und Wasserfaches (DVGW) are provided (document DVGW G 465-1 to 4 (DVGW, 2019b)). Inspections are carried out with measurement equipment (according to DVGW G 465-4 (DVGW, 2019b)) while walking along the street/areas with pipelines in the ground. Inspections of pipelines follow a fixed schedule (Table S11).

Table S11: Inspection intervals of gas pipes in the ground (Table 2 in DVGW G465-1 (DVGW, 2018))

Leak frequency (Number of detected leaks per km monitored / checked pipe	≤ 0.1	≤ 0.5	≤ 1
Operating pressure	Inspection interval in years		
≤ 1 bar	6 (only for PE-pipes and pipes with cathodic corrosion protection)	4	2
> 1 bar to ≤ 5 bar	4 (additional bimonthly track inspection)	2	1
> 5 bar to ≤ 16 bar	1 (depended on the material of the pipe)		

Leaks are classified into four categories based on proximity of the leaks to buildings, and each category requires certain actions to prevent incidents/accidents (DVGW, 2019a).

Table S12: Leak classes and action required

Leak classification	Leak detection proximity to the building	Repairing actions
A1	Leak into a building	Immediate
A2	Leak very close to a building	Within a weak
B	Leak in bigger distance to a building	3 months
C	There is no danger of incoming gas in a building or cavity	According to recommended recovery plan

S.4.2) Measurement procedures by GasNetz Hamburg

GasNetz Hamburg uses gas detectors from Sewerin (e.g. portable Ex-Tec PM4, detection limit 1 ppm above background). The analyzer sucks in air close to the ground and a person pushes the analyzer forward while online readings are available on a screen (Figure S18), while all the local gas distribution network pipelines are available and checked on site. All the 145 reported LIs where initially checked by GasNetz Hamburg by overlapping with the network map to see if the locations are in close proximity to pipeline from the NGDN. The LIs were prioritized in classes mentioned in Table S12, and finally leak detection and repair practices were carried out. The company not only checked the reported locations by this study, but also the surrounding area including house connections, parks, gardens, etc., where pipelines are located close by.

Figure S18: Leak detection operation by GasNetz Hamburg

Table S13: Distances of observed LIs from the natural gas distribution network grid

Distance (m)	Red	Orange	Yellow
0	100 %	75 %	67 %
10	----------	25 %	21 %
20	----------	----------	5 %
30	----------	----------	3 %
40	----------	----------	1 %
50	----------	----------	2 %

Table S14: Pipeline materials at the locations of observed LIs

Pipeline material	Red	Orange	Yellow
Steel	100 %	67 %	63 %
Polyethylene	----------	33 %	37 %

S.5) Gas Leak detection and repair

Mobile measurements provide enormous and valuable amount of data in a short period of time with an ability of large coverage in urban area for the purpose of detecting and quantifying leaks from NGDNs. This study shows that CH_4 mobile measurements associated with several attribution techniques are capable of distinguishing fossil LIs. In this study, we added source attribution techniques to an algorithm which was initially designed to detect and quantify leaks from pipeline. This algorithm was introduced in von Fischer et al. (2017), and later improved in Weller et al. (2019); Figure S8 shows the steps we followed in this study to detect, quantify, and attribute CH_4 emissions in urban area. We concluded that the attribution techniques we used to distinguish fossil-related sources are effective. Mobile CO_2 and C_2H_6 enhancements to eliminate non-fossil LIs is effective in locating the most potential signals related which indicate leaks from pipelines. Analyzing isotopic samples ($\delta^{13}C$ and δD) provides detailed information on the origin of emission sources, however it is time-consuming effort and not possible to take samples from all locations where we observed CH_4 enhancements. In Figure S19, we provide a flowchart based on the findings of this study and experiences we obtained by collaboration with GasNetz Hamburg and STEDIN Utrecht to locate NGDNs leaks. In this flowchart we suggest to combine mobile measurements and attribution (blue box) to report potential gas leaks to local utilities before current repair practice (green box).

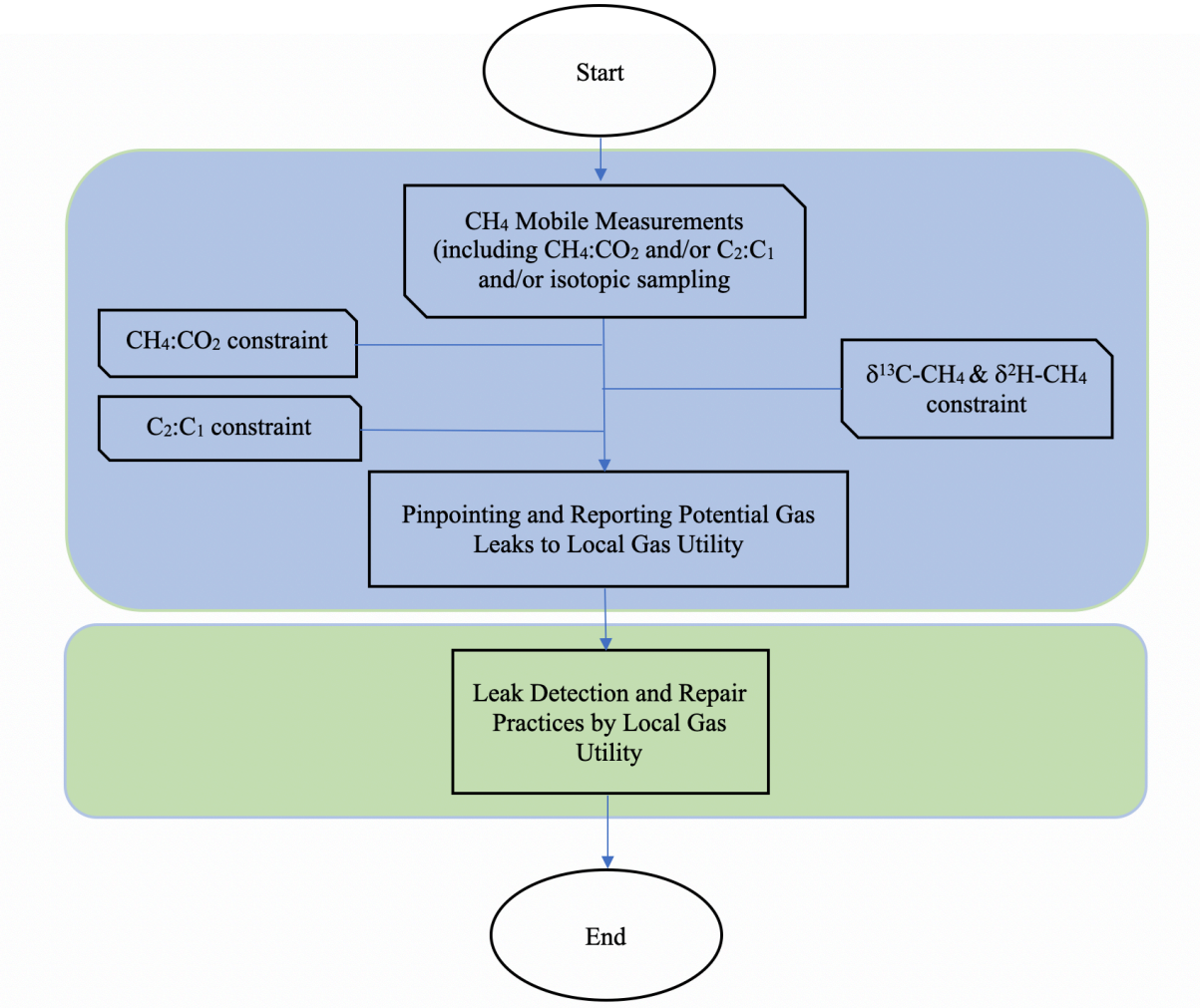

Figure S19: Gas detection and repair practices flowchart

References in SI

Bright, E. A., Coleman, P. R. and Dobson, J. E.: LandScan : A Global Population database for estimating populations at risk, [online] Available from: https://www.semanticscholar.org/paper/LandScan-%3A-A-Global-Population-database-for-at-risk-Bright-Coleman/17e6076b6761788684434d1e14e85e8877fc0146 (Accessed 23 September 2019), 2000.

DVGW: Technische Regel-Arbeitsblatt; DVGW G465-1 (A). [online] Available from: https://shop.wvgw.de/var/assets/leseprobe//510544_lp_G 465-1_2019_05.pdf, 2018.

DVGW: Technische Mitteilungen Hinweis; DVGW G 465-3. [online] Available from: https://shop.wvgw.de/var/assets/leseprobe//510545_lp_G 465-3_2019_05.pdf, 2019a.

DVGW: Technischer Hinweis - Merkblatt; DVGW G465-4 (M). [online] Available from: https://shop.wvgw.de/var/assets/leseprobe//510546_lp_G 465-4_2019_05.pdf, 2019b.

Hopkins, F. M., Kort, E. A., Bush, S. E., Ehleringer, J. R., Lai, C.-T., Blake, D. R. and Randerson, J. T.: Spatial patterns and source attribution of urban methane in the Los Angeles Basin, J. Geophys. Res. Atmos., 121(5), 2490–2507, doi:10.1002/2015JD024429, 2016.

Naus, S., Röckmann, T. and Popa, M. E.: The isotopic composition of CO in vehicle exhaust, Atmos. Environ., 177, 132–142, doi:10.1016/J.ATMOSENV.2018.01.015, 2018.

Maazallahi, H., Fernandez, J. M., Menoud, M., Zavala-Araiza, D., Weller, Z. D., Schwietzke, S., von Fischer, J. C., Denier van der Gon, H., and Röckmann, T.: MATLAB® code for evaluation of Urban Surveys, Zenodo, doi: 10.5281/zenodo.3928972, 2020.